Chapter 5

Bioconjugated Gold Nanoparticle for Rapid Capture and Targeted Photothermal Lysis of Pathogenic Bacteria

Paresh Chandra Ray,* Sadia Afrin Khan, Anant Kumar Singh, Dulal Senapati, Zhen Fan, Teresa Demeritte, and Rajashekhar Kanchanapally

Department of Chemistry, Jackson State University, 1400 Lynch St., Jackson, Mississippi 39217, USA
***E-mail: paresh.c.ray@jsums.edu. Fax: 601-979-3674**

Outbreak of food poisoning by *Salmonella* and *E. coli* bacteria are very common in this world. On the other hand, multiple drug resistant *Salmonella enterica* serover typhimurium definitive type 104 (DT104) is at present an emerging threat worldwide. As a result, an ultrasensitive sensing technology for the rapid detection and new approaches for the treatment of infectious bacterial pathogens that do not rely on traditional therapeutic regimes is very urgently required in today's world. This book chapter discusses our recent report on bio-conjugated nanomaterial based strategies for the pathogen detection and photothermal applications. We have focused on the basic concepts and critical properties of the nanostructures that are useful for the pathogen sensing and killing.

Introduction

Outbreaks of waterborne and food-borne pathogens like *Escherichia coli, Staphylococcus spp. and Salmonella spp*. regularly occur in the U.S and other developed countries (*1–9*). Since food production industry is worth about 578 billion U.S. dollars, often food recalls due to the presence of food-borne

In Nanomaterials for Biomedicine; Nagarajan, Ramanathan;
ACS Symposium Series; American Chemical Society: Washington, DC, 2012.

pathogens are becoming nightmare for US economical growth (*1–9*). On the other hand, due to the biological diversity of the harmful pathogens and quite low infection dose, it is a continual challenge to prevent infectious disease outbreaks. Infection disease is responsible for approximately one-third of global mortality and billion dollars of economical loss each year (*1–15*). Since current methods for the identification of pathogenic bacteria take several days to report the correct information, there is a huge demand for the development of rapid, sensitive, and reliable assay to identify the harmful pathogens selectively with high sensitivity (*1–15*). Gold nanomaterial-enabled detection strategies, which are currently in the infant stage, may be able to fulfill the demand (*10–30*). Due to the presence of large surface area, large number of target-specific recognition element such as antibody, aptamers and peptides can be attached to gold nanomaterial surface (*30–70*). As a result, bio-conjugated gold nanoparticle can be used for several pathogens simultaneously as well as selectively even at the single bacterium level, as shown in Scheme 1. Since last four years, our group has been developing gold nanomaterials based highly sensitive assay for highly selective and sensitive sensing of different pathogens (*15*, *20–23*, *30*). Current book chapter intended to illustrate the current status of the field mainly from our laboratory and also to spur possible future research in this area for the next generation scientific community.

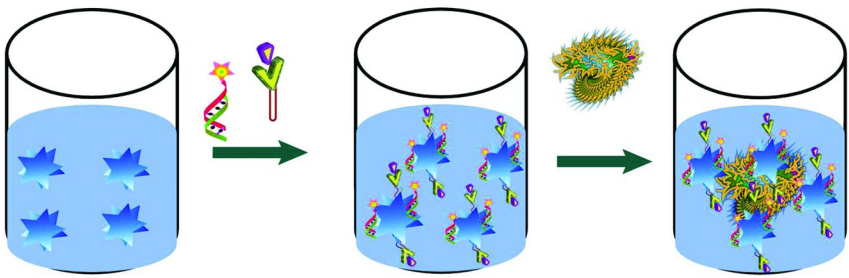

Scheme 1. Schematic representation shows bio-conjugated gold nanotechnology-driven approach to selectively capture bacteria.

Since the development of penicillin in the 1940s, antibiotics became economic powerhouses for our world society and also responsible for saving countless human lives (*1–10*). Only in the USA, there are around 42 billion U.S. dollars sales of antibiotics in 2009. It is almost 20% of drug expenditures among any therapeutic group of drugs (*1–9*). However, due to the intensive use of the antibiotics, world is now facing a tremendous problem and that is, human pathogens have become resistant to many available antibiotics (*1–10*). Multidrug resistance (MDR) in bacteria occurs by the accumulation of resistance plasmids or transposons of genes, with each coding responsible for resistance to a specific drug type (*1–10*). Due to the presence of multiple antimicrobial resistance genes

like 1) *pse* for ampicillin resistance, 2) *floR* for chloramphenicol resistance, 3) *str* for streptomycin resistance, 4) *sulI* for sulfonamide resistance, and 5) *tetR* or *tetG* for tetracycline resistance, MDR *bacteria* are resistant to five mostly used ampicillin, chloramphenicol, streptomycin, sulfonamides, and tetracycline antibiotics. As a result, MDRB became the cause for the major sources of hospital-acquired infections and approximately sixty percent of nosocomial infections (*1–10*). According to the Infectious Diseases Society of America, we must deliver 10 new antibiotics by the year 2020 and it will not be easy in this world's economical condition. Similarly, according to World Health Organization (WHO) (*9*) there may be another 1-2 decades left for people to use the existing antibiotics and after that, the MDRB infectious diseases may not be cured using currently available antibiotics in the market. All the above facts clearly indicate that the new approaches for the treatment of infectious bacterial pathogens that do not rely on traditional therapeutic regimes, is very urgent for our society's health care. One promising method, still in its infant stage, is to use nanomaterial-based photothermal killing of harmful bacteria selectively (*17–23*). We and other groups have shown that unique size and shape dependent optical properties of gold nanomaterials can be used for the selective non-invasive photothermal lysis applications for MDRB and other pathogens (*17–23*). In this book chapter, we summarize recent promising reports mainly from our group and suggest future strategies to identify, target or destroy pathogens.

Bio-Conjugated Gold Nanomaterial Based Sensing of Bacteria

Gold metal nanostructures attract much interest because they are easy to synthesize and they possess unique size or shape dependent properties (as shown in Figure 1-2), including large optical field enhancements resulting in the strong scattering and absorption of light (*10–71*). In case of noble metals, as the size is reduced to tens of nanometers scale, which is comparable to the wavelength of light, a new very strong absorption is observed, resulting from the collective oscillation of the electrons in the conduction band from one surface of the particle to the other and known as localized surface plasmon (LSP) (*10–71*). Due to the presence of LSP, electric fields near the particle's surface are greatly enhanced and the particle's optical extinction reaches maximum at the plasmon resonant frequency. It can be visible or NIR wavelength depending on size and shape of nanoparticles (*10–71*), as shown in Figure 1. Due to the huge surface plasmon enhancement, absorption cross-sections of noble gold nanoparticles are 5-7 orders of magnitude more than that of any available dye molecule (*10–71*). As a result, one can consider each metal nanoparticle as an optical probe equivalent to several million dye molecules, which will help to increase detection sensitivity tremendously (*10–71*). There is another advantage to use nanoparticle as a probe, which is, unlike dyes, metal nanoparticles are photostable and do not undergo photobleaching easily.

For biological applications, it is necessary to use near-infrared (NIR) light, especially 650−900 nm, since the absorption of physiological fluids and tissues

In Nanomaterials for Biomedicine; Nagarajan, Ramanathan;
ACS Symposium Series; American Chemical Society: Washington, DC, 2012.

and biological water is minimal in this region (*17–23*, *31–33*). One way of tuning the localized surface plasmon frequency is by changing the particle shape and size as shown in Figure 2. When an incident light couples with surface plasmon mode, it helps in the local increase of resonant electromagnetic fields over several orders of magnitude (*17–23*, *31–33*).

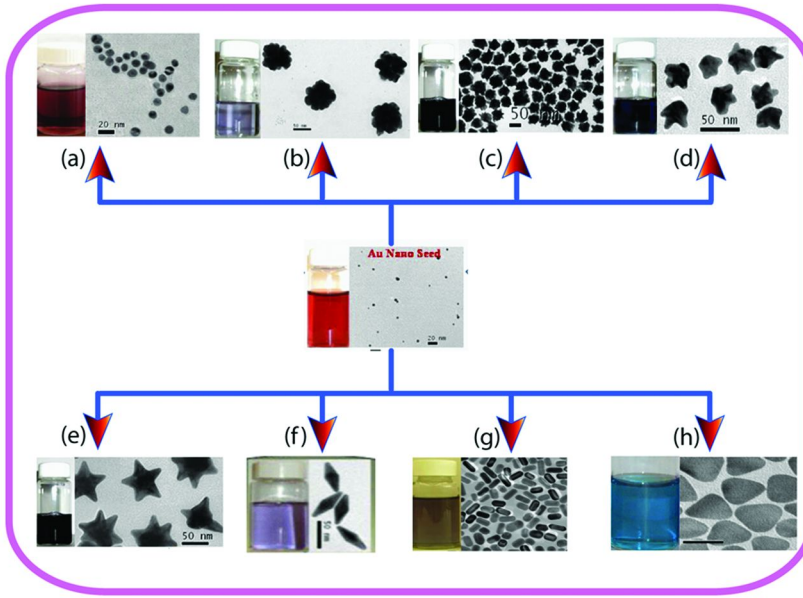

Figure 1. Picture showing how one can synthesize gold nanoparticles of different shapes from gold seed by just varying the nature and concentration of surfactant (presence of (a) 0.0 M CTAB, (b) 0.001 M CTAB, (c) 0.003 M CTAB, (d) 0.01 M CTAB, (e) 0.03 M CTAB, (f) 0.4 M CTAB, (g) 0.1 M CTAB, (h) 0.14 M CTAB.

This phenomenon enhances several radiative and non-radiative processes such as absorption, fluorescence, Raman scattering, hyper-Rayleigh scattering, and hyper-Raman scattering (*10–71*). As a result, these optical techniques have been used (*25–50*) for the recognition of pathogens by monitoring the change in the optical signal that occurs after the addition of pathogens on functionalized nanomaterials, as shown in Scheme 2. For the selective sensing and therapy, nanomaterials have been modified with different recognition elements like antibodies and aptamers to target antigen-presenting cells as epitopes present on pathogen surface (*10–25*). In the next section, we will focus on how various gold nanoparticle based surface plasmon enabled spectroscopies have been used by our groups for optical signal transduction to provide highly sensitive pathogen sensing (as shown in Scheme 2).

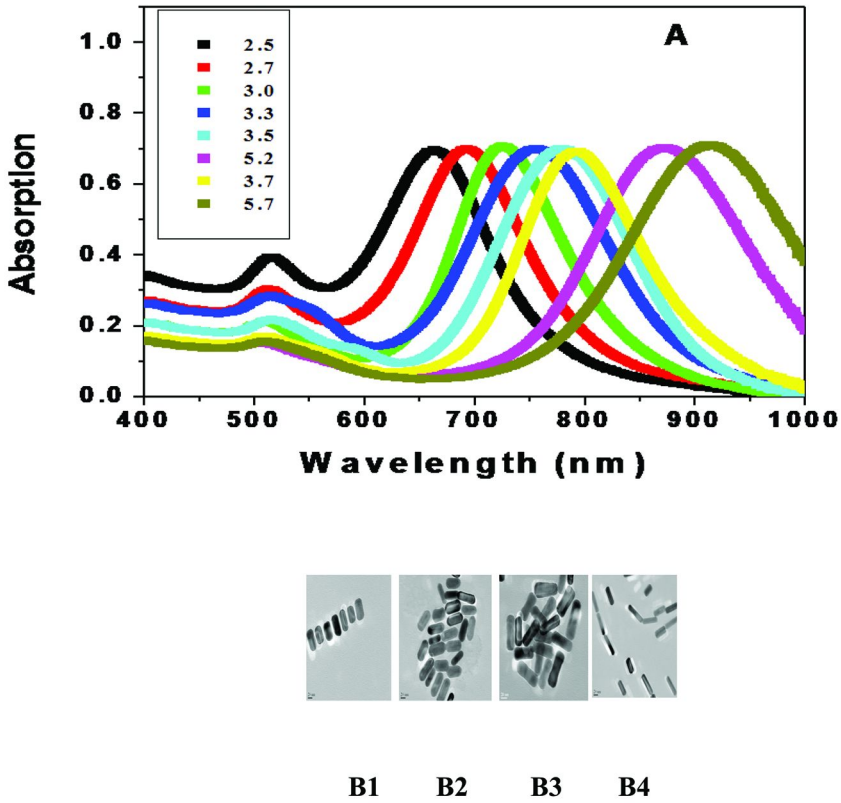

Figure 2. Extinction profile of Au nanorods with aspect ratios varying from 2.0 to 5.7 (reprinted with permission from Ref. (60), Copyright 2008, Willey- VCH). E) TEM image of gold nanorods of average aspect ratios, B1: (σ) ≈2.0, B2: (σ) ≈2.8, b3: (σ) ≈4.0 and b4: (σ) ≈5.2. (reprinted with permission from Ref. (70), Copyright 2009, Willey- VCH).

Colorimetric Bacteria Sensing

Colorimetric assay for bacteria sensing will be ideal for the development of real life biosensor, because any layman can use these sensors using naked eyes. Since the colors of gold nanoparticle solutions are highly dependent on the interparticle distance of nanoparticles, the working principle of the gold nanoparticle based colorimetric sensor is based on the fact that when individual gold nanoparticles come into close proximity, due to the interparticle plasmon coupling, a distinct color change is usually observed (*10–70*). As a result, last several years (*10–23*) we and other groups have used this colorimetric change processes for ultrasensitive bacteria sensing. In 2005, Berry et. al. (*16*)

reported that due to the strong electrostatic interactions, cetyltrimethylammonium bromide (CTAB)-functionalized gold nanorods can conformally deposit to form a monolayer on Bacillus cereus. We have reported (*20*) colorimetric detection of *E. coli* bacteria using gold nanorod. Our colorimetric bacteria identification is based on the fact that, *E. coli* bacteria are more than an order of magnitude larger in size (1−3 μm) than the anti-*E. coli* antibody-conjugated gold nanorods. In the presence of *E. coli* bacteria, several gold nanorods conjugate with one *E. coli* bacterium, as shown in Figure 3. As a result, anti-*E. coli* antibody-conjugated gold nanorods undergo aggregation (*20*). Due to the aggregation, a color change takes place (as shown in Figure 3C). This color change is mainly due the change in interparticle interaction resulting from the assembly of nanoparticles on the cell surface. This bioassay is rapid, takes less than 15 min from bacterium binding to detection and analysis, and is convenient and highly selective.

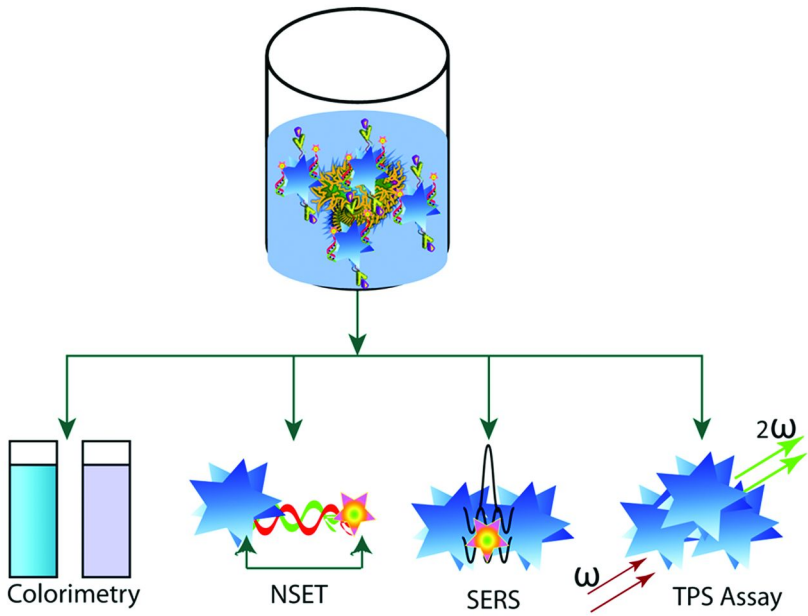

Scheme 2. Schematic representation showing different gold nanotechnology based optical techniques for the selective sensing of pathogens.

Recently we have reported (*21*) the development of bio-conjugated gold nanomaterial for the selective sensing of salmonella bacteria. For selective salmonella bacteria detection, at first we have modified the nanoparticles with anti-salmonella antibody (as shown in Figure 4A). Our reported experimental data have shown that the sensitivity of colorimetric assay for Salmonella detection

is 10^4 bacteria cells/mL (*21*), which is comparable with the detection limit (10^4–10^5cfu/mL) of ELISAs. We have also shown that gold nanoparticle based colorimetric assay is highly selective. As shown in Figure 4C, no color change has been observed even after the addition of 10^6 *E. coli* bacteria. Similarly, we have not observed any color change when we added 10^6 *Salmonella typhimurium* bacteria to anti *E. coli* antibody conjugated oval shape gold nanoparticles. On the other hand, distinct color changes have been observed when we added 10^6 *E. coli* bacteria to anti-*E. coli* antibody conjugated oval shape gold nanoparticles.

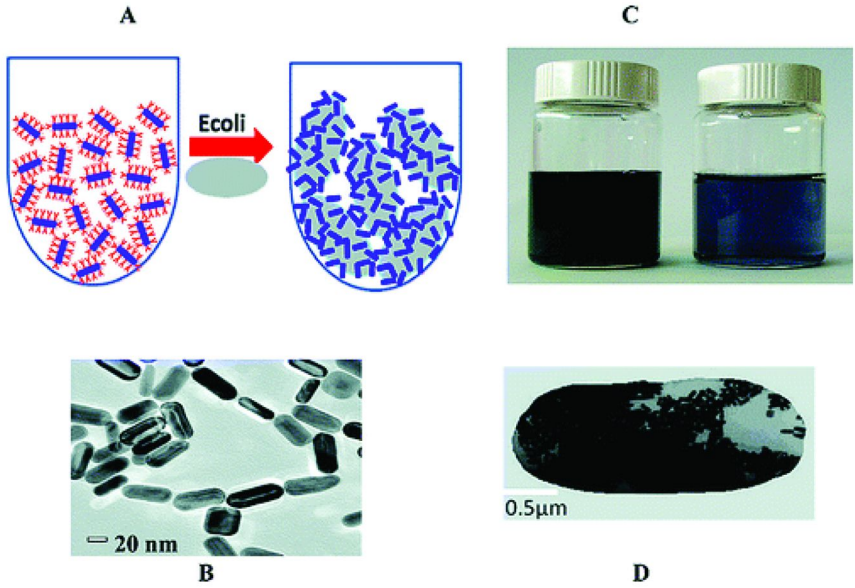

Figure 3. (A) Schematic representation of anti-E. coli antibody-conjugated nanorod-based sensing of E. coli bacteria. (B) TEM image of anti-E. coli antibody-conjugated nanorods before the addition of E. coli bacteria. (C) Photograph showing colorimetric change upon the addition of E. coli bacteria (10^4 cfu/mL), and (D) TEM image demonstrating aggregation of the gold nanorods after the addition of E. coli bacteria (10^3 cfu/mL). (reprinted with permission from Ref. (20), Copyright 2009, American Chemical Society).

Next to understand whether our gold nanotechnology based assay can detect MDRB from food sample, we have reported (*22*) the selectivity and sensitivity of our colorimetric assay using ampicillin, chloramphenicol, streptomycin, sulfonamides, and tetracycline antibiotics drug resistant (MDRB) *S. typhimurium DT104* (ATCC 700408) infected romaine lettuce. For this purpose, we purchased lettuce from Walmart and then chopped them into small pieces. After that chopped lettuces were infected them with Salmonella DT104. Figure 5 shows the

In Nanomaterials for Biomedicine; Nagarajan, Ramanathan;
ACS Symposium Series; American Chemical Society: Washington, DC, 2012.

selectivity and sensitivity of our colorimetric assay, when antibody-conjugated gold nanoparticles were mixed with various concentrations of MDRB *S. typhimurium DT104* infected lettuce samples. As shown in Figure 5, no color change has been observed even after the addition of lettuce sample infected by10^6 CFU/gm *Salmonella ser. Agona* or *E. coli* bacteria on to M3038 antibody conjugated popcorn shape gold nanoparticle. We have also tested for mixture of bacteria, as shown in Figure 5. Our result clearly shows that the color change is observed only when MDRB 10^3 CFU/gm or above *Salmonella* DT104 is present. The sensitivity of this colorimetric assay was 10^3 CFU/gm.

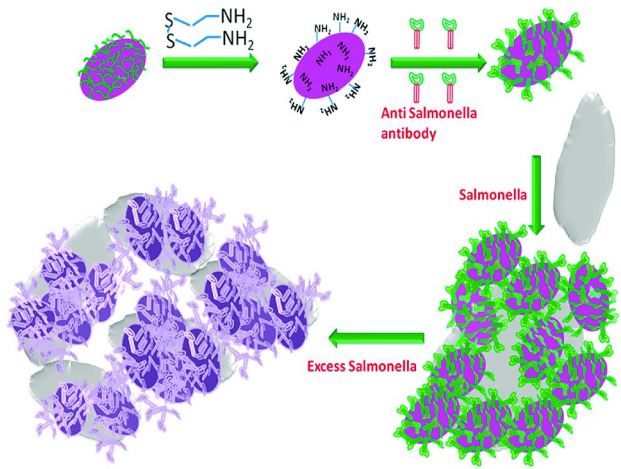

A

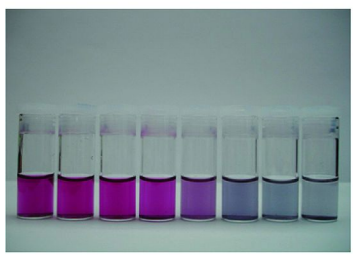

B

C

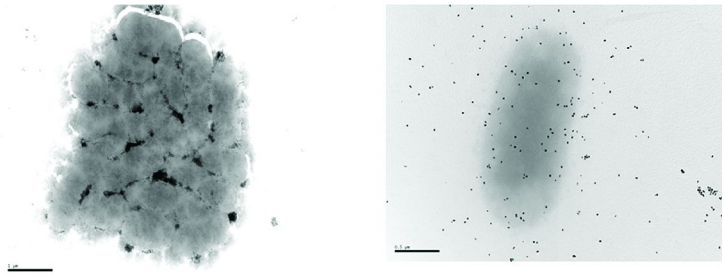

D **E**

Figure 4. A) Schematic representation showing antibody-conjugated nanotechnology-driven approach using oval shape gold nanoparticle to selectively target and destroy pathogenic bacteria. B) Photograph showing colorimetric change upon the addition of (from left to right) 10, 50, 100, 500, 1000, 5000, 10000, 50000, 100000, 500000 CFU/mL Salmonella bacteria. C) Photograph showing colorimetric change upon the addition of i) 10^6 E. coli bacteria to anti salmonella antibody conjugated oval shape gold nanoparticles, ii) 10^6 salmonella bacteria to anti E. coli antibody conjugated oval shape gold nanoparticles, iii) 10^3 E. coli bacteria to anti E. coli antibody conjugated oval shape gold nanoparticles, iv) 10^6 E. coli bacteria to anti E. coli antibody conjugated oval shape gold nanoparticles. D) TEM image demonstrating the formation of bigger microbial clusters in the presence 10^6 cfu/mL salmonella bacteria. E) TEM image of salmonella bacteria in the presence of anti E.coli antibody conjugated oval shape gold nanoparticles. Our TEM image clearly demonstrates that the S. typhimurium bacterium cells are poorly labeled by the anti-E.coli antibody coated oval shape gold nanoparticles. (reprinted with permission from Ref. (21), Copyright 2010, Willey- VCH).

Two-Photon Rayleigh Scattering Assay for Bacteria Sensing

The two-photon Rayleigh light scattering or hyper-Rayleigh scattering can be observed from fluctuations in symmetry, caused by rotational fluctuations (*20*, *30*, *39*, *41*, *42*, *48*, *70–74*). This is a second harmonic generation experiment in which the light is scattered in all directions rather than as a narrow coherent beam (*20*, *30*, *39*, *41*, *42*, *48*, *70–74*). Two-photon scattering properties of nanostructured materials are drastically influenced by the quantum confinement effect and as a result, this is highly promising for biological and chemical sensing applications (*20*, *30*, *39*, *41*, *42*, *48*, *70–74*). Recently we have demonstrated (*20*) a fast and highly sensitive assay for *E. coli* bacteria detection using an antibody-conjugated gold nanorod based two-photon scattering technique. We have reported (*20*) that when anti *E. coli* antibody-conjugated nanorods were mixed with various concentrations of *E. coli* O157:H7 bacteria, the two-photon scattering intensity increased by about 40 times. This increment is based on the fact that when anti

E. coli antibody-conjugated nanorods were mixed with various concentrations of *Escherichia coli* O157:H7 bacteria, several gold nanorods conjugated with one *E. coli* bacterium and formed bio-conjugated gold nanorod aggregates, as shown in Figure 6. As a result, the two-photon scattering intensity increased by about 40 times. Due to the aggregation in the presence of *E. coli* bacteria, nanorods lost the center of symmetry. As a result, one can expect a significant amount of electric dipole contribution to the two-photon scattering intensity. Since electric dipole contributes several times higher than that of multipolar moments, we expect two-photon scattering intensity to increase with aggregation. Again, due to the aggregation, a new broad band appears around 200 nm, far from their longitudinal plasmon absorption band, as shown in Figure 6. As a result, the single photon resonance enhancement and two-photon luminescence factors are much larger for nanorod aggregates due to the closeness of λ_{max} to the fundamental wavelength at 860 nm. This factor should increase the two-photon scattering intensity. Similarly, since size increases tremendously with aggregation, the two-photon scattering intensity is expected to increase with the increase in particle size. Our experimental results have shown that *E. coli* bacteria can be detected quickly and accurately without any amplification or enrichment at the 50 cfu/mL level with excellent discrimination against any other bacteria. Our report (*20*) clearly shows that our antibody-conjugated gold nanorod based two-photon scattering assay can provide a quantitative measurement of the *E. coli* bacteria concentration. To understand whether our assay is highly selective, we have also reported the two-photon scattering intensity changes upon the addition of *S. typhimurium* bacteria to anti-*E. coli* antibody-conjugated gold nanorods. As shown in Figure 6, two-photon scattering intensity changed by only 6% when we added the *S. typhimurium* bacteria to anti-*E. coli* antibody-conjugated gold nanorods. So our reported (*20*) data clearly show that our reported two-photon scattering assay is highly selective.

Bacteria Sensing Using Gold Nanoparticle Based SERS Assays

The possibility of observing Raman signals, which are normally very weak, with enhancements on the order of 10^8–10^{14} allow SERS to be unique for ultrasensitive pathogen sensing (*22*, *33*, *35–40*, *50–65*). Several reports show (*22*, *33*, *35–40*, *50–65*) that very high selectivity and sensitivity can be offered by SERS. Very recently, we have reported Rh-6G modified antibody-conjugated popcorn shape gold nanoparticle-based SERS technique for the detection of MDRB Salmonella DT104 (*22*). In nano-popcorn, like nano-star, the central sphere acts as an electron reservoir while the tips are capable of focusing the field at their apexes, which provides huge field enhancement of scattering signal (*22*, *33*). Our result indicates that in the presence of drug resistant MDRB *Salmonella DT104*, antibody-conjugated gold nanoparticle undergoes aggregation, which helped to form several hot spots and provided ~ 10^9 order of magnitude SERS signal enhancement through mainly electromagnetic field enhancement mechanism. Figure 7 shows the SERS enhancement in the presence of Salmonella DT104. The Raman modes at 236, 252, 273 and 376 cm^{-1} are

In Nanomaterials for Biomedicine; Nagarajan, Ramanathan;
ACS Symposium Series; American Chemical Society: Washington, DC, 2012.

N-C-C bending modes of ethylamine group of the Rh6G ring and the Raman modes at 615, 778, 1181, 1349 1366,1511, 1570, 1603 and 1650 cm^{-1} are due to C-C-C ring in-plane bending, C-H out-of-plane bending, C-N stretching and C-C stretching, as we reported (*22*, *33*). As shown in Figure 7, the SERS intensity change was negligible in the presence of 10^6 *Salmonella ser. Agona* bacteria/mL or *E.coli* bacteria, whereas a good enhancement has been observed even in the presence of only 10 CFU/gm MDRB *S. typhimurium* DT104. It is mainly due to the lack of strong interaction between antibody-conjugated popcorn shape gold nanoparticle and *Salmonella ser. Agona or E.coli* bacteria. Our reported result clearly indicates that our gold nanoparticle based SERS assay is highly selective and very sensitive.

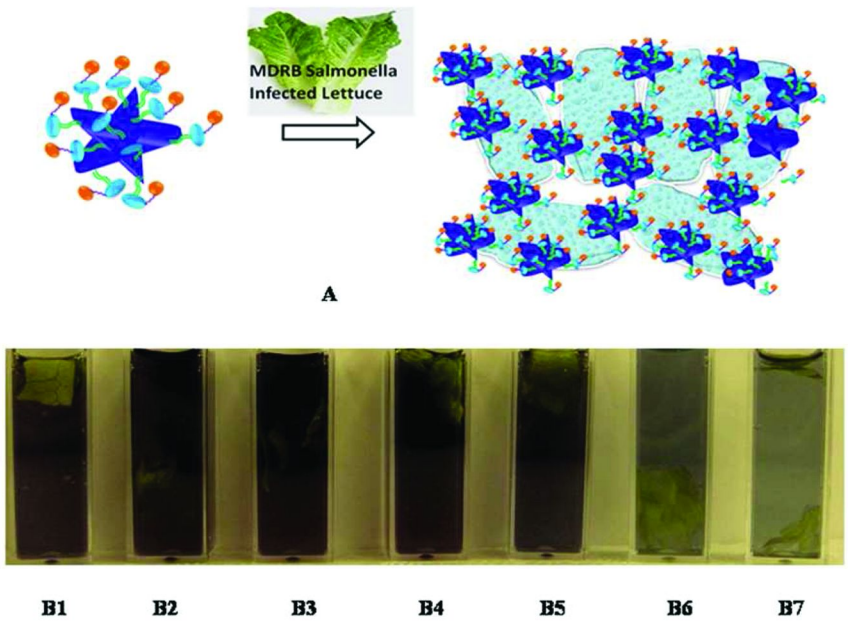

Figure 5. A) Schematic representation showing our gold nanotechnology-driven colorimetric approach for rapid selective screening of MDRB Salmonella bacteria from infected lettuce. B) Photograph showing colorimetric change upon the addition of infected lettuce on antibody-conjugated gold nanoparticle. Lettuce was infected by B1) 10^2CFU/gm MDRB Salmonella, B2) 10^6 CFU/gm Salmonella ser. Agona bacteria, B3) 10^6CFU/gm E. coli bacteria, B4) mixture of 10^6CFU/gm Salmonella ser. Agona and 10^6CFU/gm E.coli, B5) mixture of 10^6CFU/gm Salmonella ser. Agona and 10^2CFU/gm MDRB Salmonella, B6) mixture of 10^6CFU/gm Salmonella ser. Agona and 10^3CFU/gm MDRB Salmonella, B7) 10^3CFU/gm MDRB Salmonella. C) Plot demonstrating SERS enhancement (SERS intensity change before and after addition of bacteria) due to the addition of different kinds of bacteria to monoclonal M3038 antibody-conjugated popcorn shape gold nanoparticle. (reprinted with permission from Ref. (22), Copyright 2011, Royal Society).

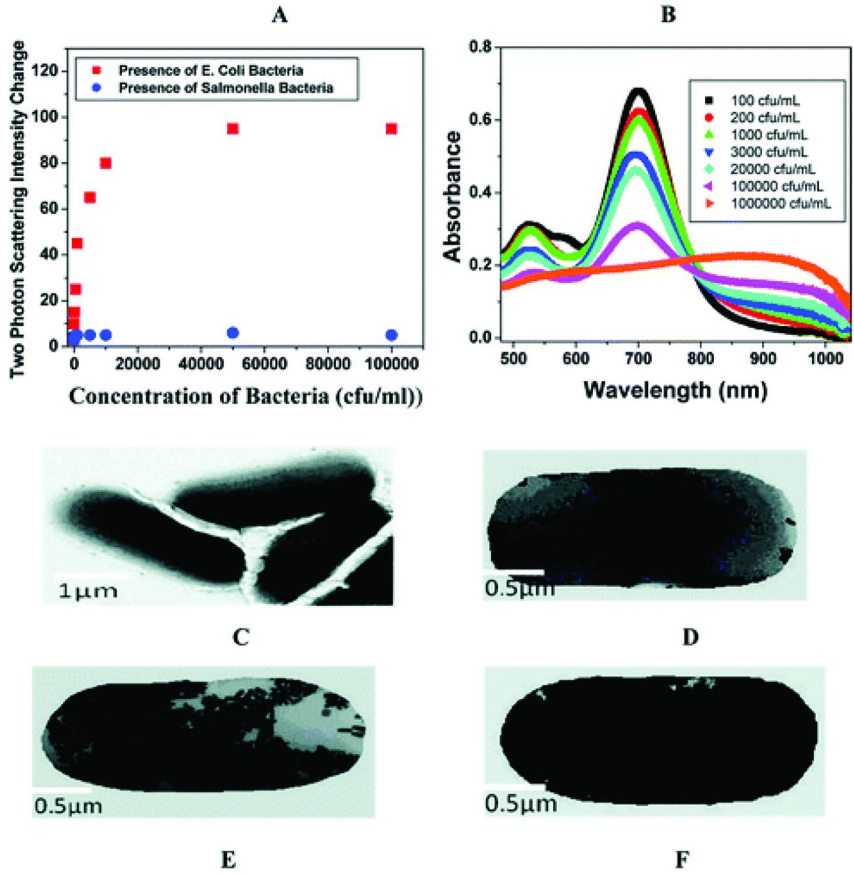

Figure 6. (A) Plot demonstrating two-photon scattering intensity changes (by 40 times) due to the addition of E. coli bacteria to anti-E. coli antibody-conjugated gold nanorods. Two-photon scattering intensity changes very little upon the addition of Salmonella bacteria. (B) Absorption profile variation of anti-E. coli antibody-conjugated Au nanorods due to the addition of different concentrations of E. coli bacteria (10^2 to 10^7 cfu/mL). The strong long wavelength band in the near-infrared region (λ_{LPR} = 680 nm) is due to the longitudinal oscillation of the conduction band electrons. The short wavelength peak ($\lambda \approx 520$ nm) is from the nanorods' transverse plasmon mode. New band appearing around 950 nm, due to the addition of E. coli bacteria, demonstrates the aggregation of gold nanorods. (C) TEM image of E. coli bacteria before the addition of nanorod. (D) TEM image after the addition of 10^2 cfu/mL E. coli bacteria. (E) TEM image demonstrating aggregation of gold nanorods after the addition of 8×10^4 cfu/mL E. coli bacteria. (F) TEM image demonstrating aggregation of gold nanorods after the addition of 10^7 cfu/mL E. coli bacteria. (reprinted with permission from Ref. (20), Copyright 2009, American Chemical Society).

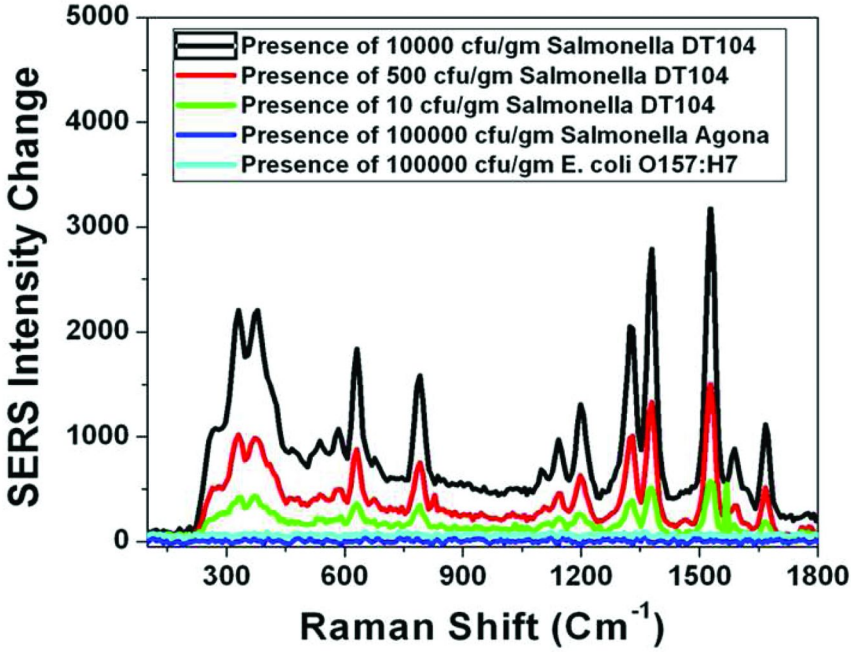

Figure 7. Plot demonstrating SERS enhancement (SERS intensity change before and after the addition of bacteria) due to the addition of different kinds of bacteria to monoclonal M3038 antibody-conjugated popcorn shape gold nanoparticle. (reprinted with permission from Ref. (22), Copyright 2011, Royal Society).

Selective Bacteria Killing Using Bio-Conjugated Gold Nanomaterial

Gold nanoparticles of different sizes and shapes with optical properties tunable in the visible to near-infrared can be used for the hyperthermic destruction of MDRB using NIR light (*17–23*), as shown in Scheme 3. For photothermal destruction, gold nanoparticles serve as "light-directed nano heaters", which is very useful for selective laser photothermolysis pathogens (*15–23*, *30–33*, *38*). Gold nanoparticles are known to absorb light several millions of times stronger than the organic dye molecules, as a result, in the presence of light of proper wavelength, due to the electron–phonon relaxation process, temperature rises on the order of a few tens of degrees (*15–23*, *30–33*, *38*). This photothermal hypothermia process produces sufficient heat for the destruction of MDRB via cell damage using different thermal effects, such as denaturation of proteins/enzymes, induction of heat-shock proteins, metabolic signaling disruption, endothelial swelling, microthrombosis, etc. (*15–23*, *30–33*, *38*). When the incident laser frequency overlapped with the plasmon absorption maximum of the gold nanoparticles conjugated pathogens, selective heating and destruction of MDRB can be achieved at a much lower laser powers than that required to destroy healthy

In Nanomaterials for Biomedicine; Nagarajan, Ramanathan;
ACS Symposium Series; American Chemical Society: Washington, DC, 2012.

bacteria to which bio-conjugated nanoparticles do not bind specifically. Zharov et. al. (*19*) reported localized killing of *S. aureus* in vitro by combining laser and photo-thermal technique. Later, Norman et. al. (*17*) reported photothermal killing using gold nanorods that have been covalently linked with antibodies to selectively destroy *Pseudomonas aeruginosa,* which was obtained from the upper respiratory tract of sinusitis patients.

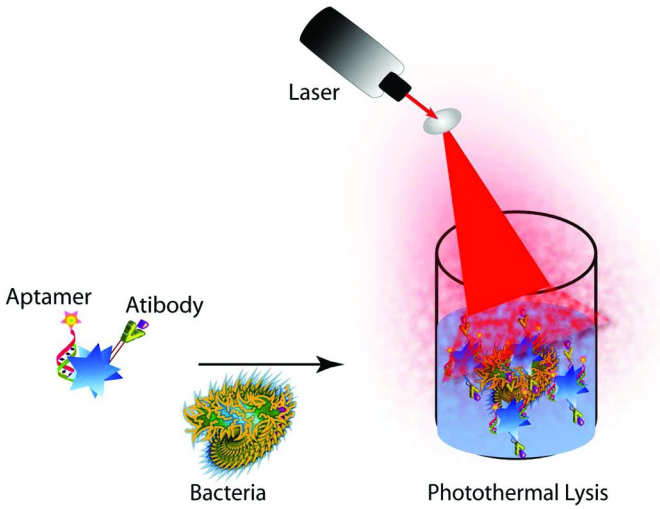

Scheme 3. Schematic representation showing bacteria conjugated nanoparticle based photothermal hyperthermic destruction for MDRB.

All initial studies did not demonstrate the selectivity of their assay with respect to other pathogens, which is very important before this technique can be used for real life sample. At 2010, we have reported selective photothermal killing of salmonella bacteria using antibody conjugated popcorn shape gold nanoparticle (*21*). As shown in Figure 8, our result shows that when oval shape gold nanoparticles are attached to bacterial cells, the localized heating that occurs during 670 nm irradiation is able to cause irreparable cellular damage. To understand whether our oval shape gold nanoparticle based photo thermal lysis assay is highly selective, we have also performed experiments to find out how our assay responds to the addition of 10^6/ml *E. coli* bacteria to anti salmonella antibody conjugated oval shape gold nanoparticle. As shown in Figure 8, most of the *E. coli* bacteria remain alive even after 15 minutes of irradiation using 670 nm light. On the other hand, 97% bacteria are killed when we use salmonella bacteria instead of *E. coli* bacteria. So our experimental results clearly show that our bioconjugated oval shape gold nanoparticle based photo-thermal lysis process is highly selective (*21*).

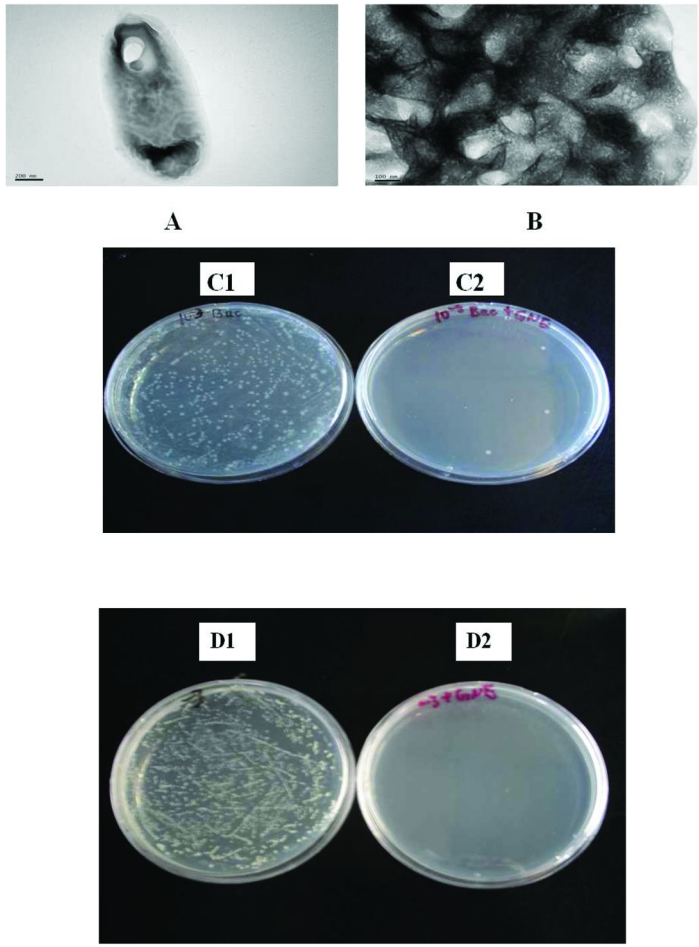

Figure 8. TEM image demonstrating irreparable damage of single bacterial cell surface when anti–Salmonella antibody coated NP conjugated S. typhimurium bacterium were exposed to 676 nm NIR radiation for 10 minutes. B) TEM image demonstrating irreparable damage of cluster of bacterial cell surfaces when NP conjugated S. typhimurium bacterium were exposed to 676 nm NIR radiation for 10 minutes. C) Colonies of S. typhimurium bacteria demonstrating the presence of the live bacteria after exposure to 670 nm light for 10 minutes to C1) 5 x 10^4 / ml S. typhimurium bacteria without NP. C2) 5 x 10^4 / ml S. typhimurium bacteria in the presence of anti–Salmonella antibody coated NP. D) Colonies of bacteria demonstrating selectivity of our photo thermal lysis process. D1) 10^6/ml E.coli bacteria in the presence of anti–Salmonella antibody coated NP. D2) 10^6/ml S. typhimurium bacteria in the presence of anti–Salmonella antibody coated NP. (reprinted with permission from Ref. (21), Copyright 2010, Willey- VCH).

After that, to demonstrate that our gold nanotechnology based assay can kill MDRB from food sample, we have reported (*23*) a photothermal assay to kill MDRB using MDRB *Salmonella DT104* infected romaine lettuce. Table 1 shows how laser irradiation time varies with the concentration of bacteria (CFU/gm) to kill 100% MDRB from MDRB infected lettuce sample. As shown in Table 1, 100 % of bacteria can be destroyed by 6 to 30 minutes laser irradiation treatment, depending on the MDRB concentration (10^2 -10^7 CFU/gm).

Table 1. Laser irradiation time to kill 100% MDRB in lettuce samples. (reprinted with permission from Ref. (*23*), Copyright 2011, Royal Society)

Concentration of MDRB (CFU/gm) in lettuce samples	*Laser Irradiation Time (minutes) to Kill 100% Bcateria*
10^2	6
10^3	9
10^4	14
10^5	20
10^6	25
10^7	30

Conclusion and Outlooks

In this chapter, we have discussed the great potential of bio-conjugated nanomaterials for the possible application of MDRB diagnostics and photothermal treatment. We have shown that outstanding plasmonic properties of metal nanoparticles are useful for bacteria labeling, imaging and diagnosis. We have reported that bio-conjugated gold nanomaterials also can be served as "nanoscopic heaters" in the presence of suitable light, which are very useful for the selective killing of MDRB without antibiotics. Photothermal MDRB destruction strategies are completely different from conventional drug therapies, and as a result, its resistance is unlikely to happen soon. Though the use of bio-conjugated nanomaterial for MDRB sensing and killings are only just the beginning, it represents one of the highly promising areas of scientific inquiry into the biomedical clinical assay and food technology field. Since the prevalence of multiple drug resistant bacteria is on the rise, we and several other groups are continuing to explore this technology. We believe that it will likely lead to the development of exciting techniques or powerful combinations of existing ones for MDRB infection disease treatment.

While there are several advantages of using nanomaterial based assays, there still remain a number of challenges which needs to be solved before it will be useful for MDRB treatment. Problems such as nonspecific binding, aggregation, and environmental stability need to be addressed, before it can be used for

In Nanomaterials for Biomedicine; Nagarajan, Ramanathan;
ACS Symposium Series; American Chemical Society: Washington, DC, 2012.

sensing in complex environments with high background and the presence of competing targets. In parallel, and for each study, toxicity and side effects need to be addressed in a serious and systematic way as a function of nanoparticle size, shape, and surface coating. As a result, an understanding of biological response and environmental remediation is necessary before they can be used as new drug. Similarly, advancement in theoretical studies at nano-bio interfaces would be of great value and will probably need to grow rapidly as new and challenging experimental results are reported.

Acknowledgments

Dr. Ray thanks NSF-PREM grant # DMR-0611539, NSF-CREST grant # HRD-0833178 and NSF-RISE grant # HRD-1137763 for their generous funding

References

1. Nikaido, H. Multidrug Resistant in Bacteria. *Annu. Rev. Biochem.* **2009**, *78*, 119–146.
2. Andersson, D. I.; Hughes, D. Antibiotic resistant and its cost: is it possible to reverse resistant? *Nat. Rev.* **2010**, *8*, 260–271.
3. Ronholm, J.; Zhang, Z.; Cao, X.; Lin, M. Monoclonal Antibodies to Lipopolysaccharide Antigens of Salmonella enterica serotype Typhimurium DT104. *HYBRIDOMA* **2011**, *30*, 43–52.
4. Allen, H. K.; Donato, J.; Wang, H. H.; Cloud-Hansen, K. A.; Davies, J.; Handelsman, J. Call of the wild: antibiotic resistant genes in natural environments. *Nat. Rev. Microbiol.* **2010**, *8*, 251–259.
5. Chiu, C. H.; Su, L. H.; Chu, C. H.; Wang, M. H.; Yeh, C. M.; Weill, F. X.; Chu, C. Detection of Multidrug-Resistant Salmonella enterica Serovar Typhimurium Phage Types DT102, DT104, and U302 by Multiplex PCR. *J. Clin. Microbiol.* **2006**, *44*, 2354–2358.
6. Pignato, S.; Coniglio, M. A.; Faro, G.; Lefevre, M.; Weill, F.-X.; Giammanco, G. Molecular Epidemiology of Ampicillin Resistance in Salmonella spp. and Escherichia coli from Wastewater and Clinical Specimens. *Foodborne Pathog. Dis.* **2010**, *7*, 945–951.
7. Perron, G. G.; Quessy, S.; Letellier, A.; Bell, G. Genotypic diversity and antimicrobial resistance in asymptomatic *Salmonella enterica* serotype Typhimurium DT104. *Infect., Genet. Evol.* **2007**, *7*, 223–228.
8. Cabello, F. C. Aquaculture and florfenicol resistance in *Salmonella enterica* serovar Typhimurium DT104. *Emerging Infect. Dis.* **2009** (April), available from http://wwwnc.cdc.gov/eid/article/15/4/08-1171.htm.
9. World Health Organization, Tuberculosis (TB). Available from http://www.who.int/tb/challenges/mdr/en/index.html (accessed October 10, 2010).
10. Ram, S.; Vajpayee, P.; Shanker, R. Prevalence of Multi-Antimicrobial-Agent Resistant, Shiga Toxin and Enterotoxin Producing *Escherichia coli* in Surface Waters of River Ganga. *Environ. Sci. Technol.* **2007**, *41*, 7383–7388.

11. Smith, P. Aquaculture and florfenicol resistance in *Salmonella enterica* Typhimurium DT104. *Emerging Infect. Dis.* **2008**, *14*, 1327–8.
12. Patel, J. R.; Bhagwat, A. A.; Sanglay, G. C.; Solomon, M. B. Rapid detection of Salmonella from hydrodynamic pressure-treated poultry using molecular beacon real-time PCR. *Food Microbiol.* **2006**, *23*, 39–46.
13. Andersson, D. I. The biological cost of mutational antibiotic resistance: Any practical conclusions? *Curr. Opin. Microbiol.* **2006**, *9*, 461–465.
14. Vikesland, J.; Wigginton, K. R. Nanomaterial Enabled Biosensors for Pathogen Monitoring - A Review, Peter. *Environ. Sci. Technol.* **2010**, *44*, 3656–3669.
15. Khan, S. A.; Singh, A. K.; Senapati, D.; Fan, Z.; Ray, P. C. Nanomaterial for Targeted Detection and Photothermal Killing of Bacteria. *Chem. Soc. Rev.* **2012**in press.
16. Berry, V.; Gole, A.; Kundu, S.; Murphy, C. J.; Saraf, R. F. Deposition of CTAB-Terminated Nanorods on Bacteria to Form Highly Conducting Hybrid Systems. *J. Am. Chem. Soc.* **2005**, *127*, 17600–17602.
17. Norman, R. S.; Stone, J. W.; Gole, A.; Murphy, C. J.; Sabo-Attwood, T. L. Targeted Photothermal Lysis of the Pathogenic Bacteria, *Pseudomonas aeruginosa*, with Gold Nanorods. *Nano Lett.* **2008**, *8*, 302–306.
18. Wang, C.; Irudayaraj, J. Gold Nanorod probe for the Detection of Multiple Pathogens. *Small* **2008**, *4*, 2204–2208.
19. Zharov, V. P.; Mercer, K. E.; Galitovskaya, E. N.; Smeltzer, M. S. Photothermal Nanotherapeutics and Nanodiagnostics for Selective Killing of Bacteria Targeted with Gold Nanoparticles. *Biophys J.* **2006**, *90*, 619–627.
20. Singh, A. K.; Senapati, D.; Wang, S.; Griffin, J.; Neely, A.; Candice, P.; Naylor, K. M.; Varisli, B.; Kalluri, J. R.; Ray, P. C. Gold Nanorod Based Selective Identification of *Escherichia coli Bacteria* Using Two-Photon Rayleigh Scattering Spectroscopy. *ACS Nano* **2009**, *3*, 1906–1912.
21. Wang, S.; Singh, A. K.; Senapati, D.; Neely, A.; Yu, H.; Ray, P. C. Rapid Colorimetric Identification and Targeted Photothermal Lysis of Salmonella Bacteria by Using Bioconjugated Oval-shaped Gold Nanoparticles. *Chem. Eur. J.* **2010**, *16*, 5600–5606.
22. Khan, S. A.; Singh, A. K.; Senapati, D.; Fan, Z.; Ray, P. C. Targeted highly sensitive detection of multi-drug resistant salmonella DT104 using gold nanoparticles. *Chem. Commun* **2011**, *47*, 9444–9446.
23. Khan, S. A.; Singh, A. K.; Senapati, D.; Fan, Z.; Ray, P. C. Targeted highly sensitive detection of multi-drug resistant salmonella DT104 using gold nanoparticles. *J. Mater. Chem.* **2011**, *21*, 17705–17709.
24. Donath, E. Biosensors: Viruses for Ultrasensitive Assays. *Nat. Nanotech.* **2009**, *4*, 215–216.
25. Ravindranath, S. O.; Mauer, J. L.; Deb-Roy, C.; Irudayaraj, J. Biofunctionalized Magnetic Nanoparticle Integrated Mid-Infrared Pathogen Sensor for Food Matrixes. *Anal. Chem.* **2009**, *81*, 2840–2846.
26. Liu, X.; Dai, Q.; Austin, L.; Coutts, J.; Knowles, G.; Zou, J.; Chen, H.; Huo, Q. One-Step Homogeneous Immunoassay for Cancer Biomarker Detection Using Gold Nanoparticle Probes Coupled with Dynamic Light Scattering. *J. Am. Chem. Soc.* **2008**, *130*, 2780–2782.

27. Golightly, R. S.; Doering, W. E.; Natan, M. J. Surface-Enhanced Raman Spectroscopy and Homeland Security: A Perfect Match? *ACS Nano* **2009**, *3*, 2859–2869.
28. Kell, A. J.; Stewart, G.; Ryan, S.; Peytavi, R.; Boissinot, B.; Huletsky, A.; Bergeron, M. G.; Simard, B. Vancomycin-Modified Nanoparticles for Efficient Targeting and Preconcentration of Gram-Positive and Gram-Negative Bacteria. *ACS Nano* **2008**, *2*, 1777–1788.
29. Chen, T.; Wang, H.; Chen, G.; Wang, Y.; Feng, Y.; Teo, W. S.; Wu, T.; Chen, H. Hotspot-Induced Transformation of Surface-Enhanced Raman Scattering Fingerprints. *ACS Nano* **2010**, *4*, 3087–3094.
30. Ray, P. C. Size and Shape Dependent Second Order Nonlinear Optical Properties of Nanomaterials and Their Application in Biological and Chemical Sensing. *Chem. Rev.* **2010**, *110*, 5332–5365.
31. Huang, X.; El-Sayed, I. H.; Qian, W.; El-Sayed, M. A. Cancer Cell Imaging and Photothermal Therapy in the Near-Infrared Region by Using Gold Nanorods. *J. Am. Chem. Soc.* **2006**, *128*, 2115–2120.
32. Singh, A. K.; Lu, W.; Senapati, D.; Khan, S. A.; Fan, Z.; Senapati, T.; Demeritte, T.; Beqa, L.; Ray, P. C. Long-Range Nanoparticle Surface-Energy-Transfer Ruler for Monitoring Photothermal Therapy Response. *Small* **2011**, *7*, 2517–2525.
33. Lu, W.; Singh, A. K.; Khan, S. A.; Senapati, D.; Yu, H.; Ray, P. C. Gold Nano-Popcorn-Based Targeted Diagnosis, Nanotherapy Treatment, and In Situ Monitoring of Photothermal Therapy Response of Prostate Cancer Cells Using Surface-Enhanced Raman Spectroscopy. *J. Am. Chem. Soc.* **2010**, *132*, 18103–18114.
34. Kaittanis, C.; Santra, S.; Perez, J. M. Role of Nanoparticle Valency in the Nondestructive Magnetic-Relaxation-Mediated Detection and Magnetic Isolation of Cells in Complex Media. *J. Am. Chem. Soc.* **2009**, *131*, 12780–12791.
35. Xie, J.; Zhang, Q.; Lee, J. Y.; Wang, D. I. The Synthesis of SERS-Active Gold Nanoflower Tags for *In Vivo* Applications. *ACS Nano* **2008**, *2*, 2472–2480.
36. Rule, K. L.; Vikesland, P. J. Surface-Enhanced Resonance Raman Spectroscopy for the Rapid Detection of Cryptosporidium parvum and Giardia lamblia. *Environ. Sci. Technol.* **2009**, *43*, 1147–1152.
37. Li, F.; Zhao, Q.; Wang, C.; Lu, X.; Li, X. F.; Le, X. C. Detection of *Escherichia coli* O157:H7 Using Gold Nanoparticle Labeling and Inductively Coupled Plasma Mass Spectrometry. *Anal. Chem.* **2010**, *82*, 3399–3403.
38. Jain, P. K.; Huang, X.; El-Sayed, I. H.; El-Sayed, M. A. Noble Metals on the Nanoscale: Optical and Photothermal Properties and Some Applications in Imaging, Sensing, Biology, and Medicine. *Acc. Chem. Res.* **2008**, *41*, 1578–1586.
39. Lu, W.; Arumugam, S. R.; Senapati, D.; Singh, A. K.; Arbneshi, T.; Khan, S. A.; Yu, H.; Ray, P. C. Multifunctional Oval Shape Gold Nanoparticle Based Selective Detection of Breast Cancer Cells Using Simple Colorimetric and Highly Sensitive Two-Photon Scattering Assay. *ACS Nano* **2010**, *4*, 1739–1749.

40. Dasary, S. S. R.; Singh, A. K.; Senapati, D.; Yu, H.; Ray, P. C. Gold Nanoparticle Based Label-Free SERS Probe for Ultrasensitive and Selective Detection of Trinitrotoluene. *J. Am. Chem. Soc.* **2009**, *131*, 13806–13812.
41. Neely, A.; Perry, C.; Varisli, B.; Singh, A. K.; Arbneshi, T.; Senapati, D.; Kalluri, J. R.; Ray, P. C. Ultrasensitive and Highly Selective Detection of Alzheimer's Disease Biomarker Using Two-Photon Rayleigh Scattering Properties of Gold Nanoparticle. *ACS Nano* **2009**, *3*, 2834–284.
42. Griffin, J.; Singh, A. K.; Senapati, D.; Lee, E.; Gaylor, J.; Boone, J. J.; Ray, P. C. Sequence Specific HCV-RNA Quantification Using Size Dependent Nonlinear Optical Properties of Gold Nanoparticles. *Small* **2009**, *5*, 839–845.
43. Griffin, J.; Singh, A. K.; Senapati, D.; Rhodes, P.; Mitchell, K.; Robinson, B.; Yu, E.; Ray, P. C. Size and Distance Dependent NSET Ruler for Selective Sensing of Hepatitis C virus RNA. *Chem. Eur. J.* **2009**, *15*, 342–351.
44. Darbha, G. K.; Rai, U. S.; Singh, A. K.; Ray, P. C. Highly Selective detection of Hg^{2+} ion using NLO properties of gold nanomaterial. *J. Am. Chem. Soc.* **2008**, *130*, 8038–8042.
45. Griffin, J.; Ray, P. C. Gold Nanoparticle Based NSET For Monitoring Mg^{2+} Dependent RNA Folding. *J. Phys. Chem. B* **2008**, *112*, 11198–11201.
46. Schmucker, A. L.; Harris, N.; Banholzer, M. J.; Blaber, M. G.; Osberg, K. D.; Schatz, G. C.; Mirkin, C. A. Correlating Nanorod Structure with Experimentally Measured and Theoretically Predicted Surface Plasmon Resonance. *ACS Nano* **2010**, *4*, 5453–5463.
47. Darbha, G. K.; Ray, S.; Ray, P. C. Gold-nanoparticle-based miniaturized FRET Probe for rapid and ultra-sensitive detection of mercury in soil, water and fish. *ACS Nano* **2007**, *3*, 208–214.
48. Ray, P. C. Label-Free Diagnostics of single base-mismatch DNA hybridization on Gold Nano-particles using hyper-Rayleigh scattering technique. *Angew. Chem., Int. Ed.* **2006**, *45*, 1151–1154.
49. Wijaya, A.; Schaffer, S. B.; Pallares, I. G.; Kimberly, H.-S. Selective Release of Multiple DNA Oligonucleotides from Gold Nanorods. *ACS Nano* **2009**, *3*, 80–86.
50. Cao, Y. W. C.; Jin, R. C.; Mirkin, C. A. Nanoparticles with Raman spectroscopic fingerprints for DNA and RNA detection. *Science* **2002**, *297*, 1536–1540.
51. Nie, S.; Emory, S. R. Probing Single Molecules and Single Nanoparticles by Surface-Enhanced Raman Scattering. *Science* **1997**, *275*, 1102–1104.
52. Giljohann, D. A.; Seferos, D. S.; Prigodich, A. E.; Patel, P. C.; Mirkin, C. A. Gene regulation with polyvalent siRNA-nanoparticle conjugates. *J. Am. Chem. Soc.* **2009**, *131*, 2072–2073.
53. Porter, M. D.; Lipert, R. J.; Siperko, L. M.; Wang, G.; Narayanana, R. SERS as a bioassay platform: fundamentals, design, and applications. *Chem. Soc. Rev.* **2008**, *37*, 1001–1011.
54. Tiwari, V. S.; Oleg, T.; Darbha, G. K.; Hardy, W.; Singh, J. P.; Ray, P. C. Non-resonance SERS Effects of Silver Colloids with Different Shapes. *Chem. Phys. Lett.* **2007**, *446*, 77–82.

55. Casadi, F.; Leona, M.; Lombardi, J. R.; Van Duyne, R. Identification of Organic Colorants in Fibers, Paints, and Glazes by Surface Enhanced Raman Spectroscopy. *Acc. Chem. Res.* **2010**, *43*, 782–791.
56. Brus, L. Noble Metal Nanocrystals: Plasmon Electron Transfer Photochemistry and Single-Molecule Raman Spectroscopy. *Acc. Chem. Res.* **2008**, *41*, 1742–1749.
57. Pallaoro, A.; Braun, G. B.; Reich, N. O.; Moskovits, M. Mapping Local pH in Live Cells Using Encapsulated Fluorescent SERS Nanotags. *Small* **2010**, *6*, 618–622.
58. Baik, J. M.; Lee, S. J.; Moskovits, M. Polarized Surface-Enhanced Raman Spectroscopy from Molecules Adsorbed in Nano-Gaps Produced by Electromigration in Silver Nanowires. *Nano Lett.* **2009**, *9*, 672–676.
59. Yan, B.; Thubagere, A.; Premasiri, R. W.; Ziegler, L. D.; Negro, L. D.; Reinhard, B. M. Engineered SERS Substrates with Multiscale Signal Enhancement: Nanoparticle Cluster Arrays. *ACS Nano* **2009**, *3*, 1190–1202.
60. Lu, W.; Singh, A. K.; Khan, S. A.; Senapati, D.; Yu, H.; Ray, P. C. Gold Nano-Popcorn Based Targeted Diagonosis, Nanotherapy Treatment and In-Situ Monitoring of Photothermal Therapy Response of Prostate Cancer Cells Using Surface Enhanced Raman Spectroscopy. *J. Am. Chem. Soc.* **2010**, *132*, 18103–18114.
61. Lorenzo, L. R.; Javier, F.; Abajo, G.; Liz-Marzn, L. M. Surface Enhanced Raman Scattering Using Star-Shaped Gold Colloidal Nanoparticles. *J. Phys. Chem. C* **2010**, *114*, 7336–7340.
62. Khoury, C. G.; Vo-Dinh, T. Gold Nanostars For Surface-Enhanced Raman Scattering: Synthesis, Characterization and Optimization. *J. Phys. Chem. C* **2008**, *112*, 18849–18859.
63. Hu, Y. S.; Jeon, J.; Seok, T. J.; Lee, S.; Hafner, J. H.; Drezek, R. A.; Choo, H. Enhanced Raman Scattering from Nanoparticle-Decorated Nanocone Substrates: A Practical Approach to Harness In-Plane Excitation. *ACS Nano* **2010**, *4*, 5721–5730.
64. Dondapati, S. K.; Sau, T. K.; Hrelescu, C.; Klar, T. A.; Stefani, F. D.; Feldmann, J. Label-free Biosensing Based on Single Gold Nanostars as Plasmonic Transducers. *ACS Nano* **2010**, *4*, 6318–6322.
65. Song, H. M.; Wei, Q.; Ong, Q. K.; Wei, A. Plasmon-Resonant Nanoparticles and Nanostars with Magnetic Cores: Synthesis and Magnetomotive Imaging. *ACS Nano* **2010**, *4*, 5163–5173.
66. Zelada-Guillén, G. A.; Riu, J.; Düzgün, A.; Rius, F. X. Immediate Detection of Living Bacteria at Ultralow Concentrations Using a Carbon Nanotube Based Potentiometric Aptasensor. *Angew. Chem., Int. Ed.* **2009**, *48*, 7334–7337.
67. Antoine, I. R.; Benichou, E.; Bachelier, G.; Jonin, C.; Brevet, P. F. Multipolar Contributions of the Second Harmonic Generation from Silver and Gold Nanoparticles. *J. Phys. Chem. C* **2007**, *111*, 9044–9048.
68. Dadap, J. I.; Shan, J.; Eisenthal, K. B.; Heinz, T. F. Second-Harmonic Rayleigh Scattering from a Sphere of Centrosymmetric Materials. *Phys. Rev. Lett.* **1999**, *83*, 4045.

69. Chandra, M.; Indi, S.; Das, P. K. Depolarized Hyper-Rayleigh Scattering from Copper Nanoparticles. *J. Phys. Chem. C* **2007**, *111*, 10652–10656.
70. Darbha, G. K.; Rai, U. S.; Singh, A. K.; Ray, P. C. Gold Nanorod Based Sensing of Sequence Specific HIV-1 Virus DNA Using Hyper Rayleigh Scattering Spectroscopy. *Chem. Eur. J.* **2008**, *14*, 3896–3903.
71. Duboisset, I. R.-A.; Benichou, E.; Bachelier, G.; Jonin, C.; Brevet, P. F. Single Metallic Nanoparticle Sensitivity with Hyper Rayleigh Scattering. *J. Phys. Chem. C* **2009**, *113*, 13477–13481.
72. Clays, K.; Persoons, A. Hyper-Rayleigh Scattering in Solution. *Phys. Rev. Lett.* **1991**, *66*, 2980–2983.
73. Terhune, R. W.; Maker, P. D.; Savage, C. M. Measurements of Nonlinear Light Scattering. *Phys. Rev. Lett.* **1965**, *14*, 681.
74. Reeve, J. E.; Collins, A. H.; Mey, K. D.; Kohl, M. M.; Thorley, K. T.; Paulsen, O.; Clays, K.; Anderson, H. L. Modulated Conjugation as a Means of Improving the Intrinsic Hyperpolarizability. *J. Am. Chem. Soc.* **2009**, *131*, 2758–2759.